Title

The Genetic Heterogeneity among Different Mouse Strains Impacts the Lung Injury Potential of Multiwalled Carbon Nanotubes

Journal

Small, 13(33)

ISSN

1613-6810

Authors

Wang, Xiang

Liao, Yu-Pei

Telesca, Donatello

et al.

Publication Date

2017-09-01

DOI

10.1002/smll.201700776

Peer reviewed

HHS Public Access

Author manuscript

Small. Author manuscript; available in PMC 2018 September 01.

Published in final edited form as:

Small. 2017 September ; 13(33): . doi:10.1002/smll.201700776.

The Genetic Heterogeneity among Different Mouse Strains Impacts the Lung Injury Potential of Multi-walled Carbon Nanotubes

Xiang Wang[†,‡], **Yu-Pei Liao**[†], **Donatello Telesca**[§], **Chong Hyun Chang**[‡], **Tian Xia**[†,‡], and **André E. Nel**[†,‡,*]

[†]Department of Medicine, Division of NanoMedicine, University of California, Los Angeles, CA 90095, United States

[‡]California NanoSystems Institute, University of California, Los Angeles, CA 90095, United States

[§]Department of Biostatistics, University of California, Los Angeles, CA 90095, United States

Abstract

Genetic variation constitutes an important variable impacting the susceptibility to inhalable toxic substances and air pollutants, as reflected by epidemiological studies in humans and differences among animal strains. While multi-walled carbon nanotubes (MWCNTs) are capable of causing lung fibrosis in rodents, it is unclear to what extent the genetic variation in different mouse strains influence the outcome. We chose four inbred mouse strains, including C57Bl/6, Balb/c, NOD/ShiLtJ and A/J, to test the pro-fibrogenic effects of a library of MWCNTs *in vitro* and *in vivo*. *Ex vivo* analysis of IL-1β production in bone marrow-derived macrophages (BMDMs) as molecular initiating event (MIE) were performed. The order of cytokine production (Balb/c > A/J > C57Bl/6 > NOD/ShiLtJ) in BMDMs was also be duplicated during assessment of IL-1β production in the bronchoalveolar lavage fluid of the same mouse strains 40 hr after oropharyngeal instillation of a representative MWCNT. Animal test after 21 days also confirmed a similar hierarchy in TGF-β1 production and collagen deposition in the lung. Statistical analysis confirmed a correlation between IL-1β production in BMDM and the lung fibrosis. All considered, these data demonstrate that genetic background indeed plays a major role in determining the pro-fibrogenic response to MWCNTs in the lung.

Table of Content

[*]Corresponding Author: André E. Nel, M.D./Ph.D., Department of Medicine, Division of NanoMedicine, UCLA School of Medicine, 52-175 CHS, 10833 Le, Conte Ave, Los Angeles, CA 90095-1680. Tel: (310) 825-6620, Fax: (310) 206-8107, anel@mednet.ucla.edu.

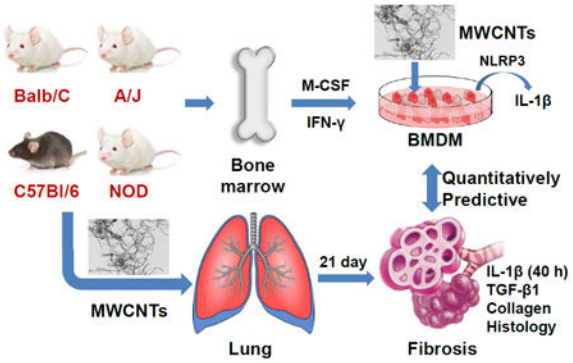

Keywords

MWCNT; BMDM; Mouse Strain; Lung Fibrosis

Due to their high tensile strength, conductivity, and light weight, there is increasing commercial use and inclusion of carbon nanotubes (CNTs) in consumer products.[1-2] However, this upward trend could be stymied by the potential hazardous effects of these long aspect ratio (LAR) materials, as demonstrated by adverse pulmonary effects in rodent lungs.[3-7] A number of studies have demonstrated the propensity of LAR materials to induce lysosomal damage and oxidative stress in phagocytic cells, leading to the generation of granulomatous inflammation and fibrosis in the lungs of experimental animals following intratracheal instillation, oropharyngeal aspiration, or aerosolized inhalation.[4-5,8-22] Interestingly, the majority of these studies were conducted in popular, empirically-selected inbred mouse (e.g. C57Bl/6) or rat (e.g. Wistar) strains that may fail to capture the impact of genetic variability in an outbred human population. This also holds true for most engineered nanomaterials (with the exception of Ag, ZnO and quantum dots), where the impact of heritable genetic factors have not been comprehensively assessed in multiple rodents strains, as to undertaken for air pollution particles, ozone and cigarette smoke.[23-26] Heritable factors are also known to determine the response outcome to stimuli such as xenobiotics, including through the impact on absorption, bioavailability, distribution, metabolism, and excretion.[27] Moreover, epidemiological studies have demonstrated the importance of genetic variation on the adverse respiratory and cardiovascular responses to ultrafine particles in susceptible individuals.[28-30] It is important that the same type of testing now being performed for CNTs, which are frequently subject to the submission of safety data during pre-manufacturing notices to regulatory agencies.[31] Clarity on the preferable rodent strains to be used for data generation would be valuable information.

Although animal testing has traditionally been considered the “gold standard” for chemical safety analysis, this study approach is labor expensive, time consuming, and often provide descriptive rather than mechanistic data.[32] With the introduction of a 21st century approach to chemical safety analysis, the use of non-vertebrate testing, a.k.a. alternative test strategies (ATS), is now included in the reform of the Toxic Substances Control Act (TSCA) in the U.S.[33-34] as well as REACH provisions in Europe.[31] Thus, it is now envisaged that ATS could provide key safety data for chemicals and new chemical substances such as

nanomaterials.[31,35] Utilizing an iterative strategy, we have developed a predictive toxicological approach for CNTs wherein we have developed a series of cellular assays for predicting the pro-fibrogenic potential of carbonaceous and LAR nanomaterials in the lung.[3,9-10,36-37] The mechanistic basis of these studies is that material aspect ratio and surface catalytic properties are responsible for the generation of lysosomal damage, which can trigger the assembly of the NLRP3 inflammasome in macrophages.[32,38] This leads to early IL-1β release, which plays a role in the subsequent mesenchymal transition of alveolar epithelial cells to fibroblasts; this combination in collagen deposition in the lung under the instruction of pro-fibrogenic growth factors such as TGF-β1 and PDGF-AA.[32,38] It is possible, therefore, to use *in vitro* testing to assess IL-1β production in macrophages or myeloid cell lines as a proxy for the molecular initiating event (MIE) by which CNTs induce lysosome damage.[9] Subsequent key events (KE) in epithelial cells and fibroblasts, which can also be studied by *ex vivo* assays, include TGF-β1 and PDGF-AA production.[8,39-40] These *in vitro* assays correlate well with the fibrogenic response in the rodent lung, which can be quantitatively assessed by a biochemical assay for collagen deposition and histological staining.[3-4,9,37] All considered, the above series of events constitute a potential adverse outcome pathway (AOP), which can be used to assess the lung injury potential of CNTs based on physicochemical properties such as wall number, length, purity, metal contamination, agglomeration, surface functionality, defects, hydrophobicity, etc.[10,21,34] Because there are a number of heritable diseases in humans where mutations of components of the NLRP3 pathway can lead to the development of immune mediated febrile illnesses,[41-43] we hypothesized studying the same pathway in different mouse strains could help to elucidate the role of genetic variation in the lung injury response.

We obtained four genetically diverse inbred mouse strains, C57Bl/6, Balb/c, NOD/ShiLtJ and A/J, to compare the pro-fibrogenic effects of MWCNTs provided by the National Institute of Environmental Health Sciences (NIEHS) Centers for Nanotechnology Health Implications Research (NCNHIR) Consortium. While C57Bl/6 and Balb/c are the most frequently used laboratory-bred strains to study mammalian lung disease, the A/J inbred strain is widely used for cancer and immunological research, including for the assessment of acute inflammation by xenobiotics.[24] In contrast, NOD/ShiLtJ is a diabetes-prone inbred strain.[44] Primary bone marrow-derived macrophages (BMDMs) were prepared from these strains and used for quantitative comparison of IL-1β production by MWCNTs. Subsequently, a representative MWCNT was chosen for comparative *in vivo* studies on the pro-fibrogenic response in the lung. The data demonstrate excellent correlation of the variances in BMDM-derived IL-1β production among the murine strains with the pro-fibrogenic injury responses in the lung.

RESULTS

Physicochemical characterization of MWCNTs

A series of 9 MWCNTs were provided by the NCNHIR consortium, and characterized by the Nanotechnology Cancer Laboratory at the US National Cancer Institute, where these materials were divided into 3 different categories based on size: (i) MWCNTs with an outer diameter of 10-20 nm and length of 0.5-2 μm (NIEHS-12); (ii) MWCNTs with an outer

diameter of 30-50 nm and length of 0.5-2 μm (NIEHS-13); and (iii) MWCNTs with a diameter of 10-20 nm and length of 10-30 μm (NIEHS-14). In addition to the as-purchased (AP) samples provided by the manufacturer (Cheap Tubes, Inc.), the materials were also used to derive carboxyl (COOH) functionalized MWCNTs (NIEHS-12-2, NIEHS-13-2, NIEHS-14-2), as well as acid-purified (PD) samples (NIEHS-12-3, NIEHS-13-3, NIEHS-14-3). Our own TEM analysis confirmed that the materials had similar ultrastructural features (Figure 1A), and that elemental analysis using the SEM-EDS feature showed a carbon purity of 89-94% for all the materials (Table 1) The major metal impurities were Ni and Fe, which did not differ appreciably among the different tube samples (Table 1). Endotoxin levels were determined by a Limulus Amebocyte Lysate assay (Lonza, Walkersville, MD), which showed while the 3 carboxyl-functionalized tubes had endotoxin levels ~1.25 EU/mL, the corresponding values for AP- and PD-MWCNTs were <1 EU/mL (Figure S1). Assessment of the hydrodynamic size by dynamic light scattering (HT-DLS, Dynapro Plate Reader, Wyatt Technology) showed diameters of 226.6 to 650.9 nm for the AP- and PD- tubes in DI water, while the same parameter for the COOH-tubes varied from 105.8 to 171.7 nm. The corresponding hydrodynamic size ranges in complete RPMI medium (containing 10 % FBS) were similar to the values for DI H_2O (Table 1). The zeta potentials of the MWCNTs ranged from –10.3 to –16.0 mV in cell culture media and –22.4 to –26.9 mV in water for AP- and PD-MWCNTs, and around -50 mV for COOH-tubes (Table 1).

As-prepared- and acid purified-MWCNTs induce *in vitro* pro-fibrogenic responses

Prior to screening primary bone marrow derived macrophages (BMDM), differentiated myeloid (THP-1) and transformed lung epithelial cell lines (BEAS-2B) were used to screen for IL-1β and TGF-β1 production in response to the MWCNTs. These are two portal-of-entry cell types that mimic the mechanistic injury responses to LAR materials in pulmonary macrophages and alveolar epithelial cells during exposure to MWCNTs.[5,33,45] Lysosome damage in THP-1 cells leads to the assembly of the NRLP3 inflammasome and IL-1β production.[5,19,32-33,45] In contrast, BEAS-2B cells mimic the epithelial response by the production of a pro-fibrogenic growth factor, TGF-β1.[37,39] Cytotoxicity assays prior to screening for cytokine and growth factor production did not show a significant decrease in cell viability in contrast to the lethal effect of nano-ZnO, used as a positive control (Figure S2A, B). Screening for IL-1β production in the supernatants of THP-1 cells by ELISA demonstrated an increase in cytokine production for all the tubes tested over the dose range 12.5-100 μg/mL (Figure 2A). The response of the carboxylated tubes was less than AP and acid-purified MWCNTs. Monosodium urate (MSU), as a LAR control, induced, and even more robust response. While the magnitude of TGF-β1 production in BEAS-2B cells was less than that of IL-1β in THP-1 cells (Figure 2B), the trend was similar (Figure 2B). IL-1β production by macrophages and TGF-β1 production by epithelial cells constitute key events (KE) in the lung fibrosis AOP by LAR materials.[40]

MWCNT exert differential pro-fibrogenic effects in BMDMs from different mouse strains

It is known that different mouse strains have differential sensitivities to xenobiotics and nanomaterials in the lung.[24] In order to compare the potential pro-fibrogenic effects of MWCNTs in different mouse strains, bone marrow-derived macrophages (BMDMs) were isolated from C57Bl/6, Balb/c, NOD/ShiLtJ and A/J mice for *ex vivo* screening of IL-1β

production. Flow cytometry was used to show that that >98% of the BMDMs express the surface markers, CD11b and F4/80 (Figure S3). Subsequent use of an IL-1β assay demonstrated a reproducible cytokine response to MWCNT exposure for individual tube types and the different mouse strains (Figure 3A). The 14-1 tube variant was used as representative material to calculate the fold-increase in IL-1β production for each strain to account for differences in the basal level of cytokine production; this demonstrated a reproducible ranking order for normalized IL-1β levels among the mouse strains (Figure 3B). Thus, while BMDMs from Balb/c mice showed the highest response, NOD/ShiLtJ mice were the least responsive, with the A/J and C57Bl/6 strains ranking in between (Figure 3B). Overall, this resulted in a ranking order of Balb/c > A/J > C57Bl/6 > NOD/ShiLtJ (Figure 3B). Interestingly, the same hierarchical ranking was also obtained during the use of positive control LAR material, MSU (Figure 3B). The *ex vivo* assessment clearly suggests that there are strain-dependent differences in the macrophage response to MWCNTs, prompting us to also study strain-dependent response differences *in vivo*.

MWCNTs induce strain-dependent differences in pro-fibrogenic effects in the lung

The 14.1 MWCNT sample was used to perform oropharyngeal aspiration in different mouse strains, followed by the assessment of the pulmonary effects after 40 hr and 21 days. These aspiration studies were performed with a MWCNT dose of 2 mg/kg per animal. The dose calculation is premised on reported ambient exposure levels as high as 400 μg/m^3in a MWCNT production facility.[46] If a healthy adult human subject with a ventilation rate of 10 L/min and assumed particle deposition rate of 30 % is exposed to such an environment, the cumulative dose over 32 weeks (8 h/day, 5 d/week) will be 92.16 mg. Using an alveolar surface area of 102 m^2 in a human adult, this is equivalent to a deposited dose of 903.53 μg/m^2. Assuming that the same surface area dose in a human and a mouse will generate the equivalent toxicological effects, the deposition 903.53 μg/m^2 in a human is comparable to a pulmonary surface area dose of 1.81 mg/kg in a 25 g mouse (estimated alveolar epithelial surface area of 0.05 m^2).[37,47] Based on these calculations, we chose a bolus dose of 2 mg/kg per animal. Min-U-Sil (α-quartz) was used as a positive control at 5 mg/kg; this material is a highly inflammogenic and is known to induce chronic lung inflammation and fibrosis. In the 1st experiment, mice were sacrificed at 40 h to measure IL-1β production as an early bioresponse marker in the lung. Examination of the bronchoalveolar lavage fluid (BALF) demonstrated strain-dependent differences in the IL-1β production and neutrophil infiltration in response to the 14.1 MWCNT sample as well as quartz (QTZ). While a clear cytokine response could be observed in Balb/c, C57Bl/6, and A/J mice, essentially no IL-1β increase was seen in NOD/ShiLtJ mice, which also mounted a relatively poor response to QTZ. When expressing the IL-1β response to MWCNTs relative to the basal production level, the normalized response ranking was: Balb/c > C57Bl/6 > A/J > NOD/ShiLtJ (Figure 4A and B). This is similar to the *ex vivo* ranking obtained in BMDMs. Neutrophil infiltration in the BALF roughly followed the same response profiling (Figure S4A and B), while lung histological analysis showed mild inflammation around small- and medium-sized airways (not shown).

Repetition of the same experiment, where the animals were sacrificed 21 days after a one-time bolus dose, was also carried out. Measurement of TGF-β1 in the BALF demonstrated

increased production of this pro-fibrogenic growth factor in the hierarchical order: Balb/c > C57Bl/6 > A/J > NOD/ShiLtJ (Figure 5A and B). We also performed a Sircol assay to quantitatively assess collagen production in the lung, demonstrating that the 14-1 MWCNT sample induced collagen production with the same hierarchical order as described for the different strains about (Figure 5C and D).

These results were confirmed by Masson's trichrome staining, which demonstrated the appearance of blue-stained collagen deposition around small airways that mirrors the result of the Sircol assay (Figure 5E). Quartz, used as a positive control, also induced differential collagen staining that is in accordance with the strain-dependent differences for MWCNT. H&E staining of the lung tissue also showed chronic inflammatory changes in accordance with the pro-fibrogenic effects in the lung (Figure S4C) at 21 days.

All considered, the animal cytokine and growth factor data show good agreement with the strain-dependent differences in BMDMs, as well as pro-fibrogenic changes in the lung. This was further confirmed by calculating the correlation coefficient between *ex vivo* and *in vivo* results. Data were normalized to obtain the logarithmic change between exposed vs non-exposed cellular and animal response parameters. The rescaled response parameters were then used in a two-way analysis of variance (ANOVA), in which the *ex vivo* response in BMDMs was compared to the BALF (IL-1β and TGF-β1) and collagen responses in the lung.[48] Using exchangeability assumptions, estimation of the linear correlation between *ex vivo* and *in vivo* endpoints demonstrated that strain difference and biological effects explain ~86 % of total variance. The assumption of exchangeability between outcomes, which amounts to the estimation of one correlation coefficient, is often used to characterize the sampling distribution of a multivariate outcome measure. In our setting, the assumption is simply used as a way to obtain an overall summary of *ex vivo* to *in vivo* prediction, without interfering with the validity of statistical inference. The concept of exchangeability *per se* is crucial in multivariate analysis above and beyond nanoparticle toxicity studies.[49] Table 2 depicts the differences in the MWCNT-induced pro-fibrogenic effects, showing that most of the variation occurred in the biological endpoints. Thus, 57 % of the variance is explained by differences between *ex vivo* and *in vivo* measurements, 16 % of the variance is explained by differential strain susceptibility, and the remaining 7 % was explained by the differences among *in vivo* endpoints. This point is further illustrated in Figure 6, which shows the mean log-fold changes *ex vivo* and *in vivo* for all endpoints and mouse strains. Linear correlation analysis shows a correlation coefficient of 0.57 (95% C.I. 0.001, 0.863) between *ex vivo* and *in vivo* data analysis, allowing us to draw the following principle conclusions: (i) the *in vivo* biological outcomes were consistent with one another within individual animal strains; (ii) there is overall consistency in susceptibility between ranking in BMDMs *ex vivo* and the multi-endpoint measurements *in vivo*. Strain susceptibility is the most important source of variance in the MWCNT-induced pro-fibrogenic effects, with the susceptibility ranking, yielding the following order: Balb/c > C57Bl/6 > A/J > NOD/ShiLtJ.

DISCUSSION

In this study, we selected a diverse group of four genetically inbred mouse strains to determine their strain-specific sensitivity to MWCNT-induced cytokine and growth factor

production, leading to an apical outcome of lung fibrosis. We demonstrate that MWCNT-triggered pro-fibrogenic changes takes place in the order Balb/c > C57Bl/6 ≈ A/J > NOD/ShiLtJ. The *ex vivo* assays, using BMDM cell cultures, correlated well with the *in vivo* results. Our findings indicate that genetic background plays an important role in MWCNT-induced pro-fibrogenic effects, implying that the choice of the mouse strain is an important consideration in planning MWCNT toxicity studies.

The major finding in this study is that genetic background plays a major role in the biological events that underpins the pro-fibrogenic potential of MWCNTs in the murine lung. Many studies that have demonstrated the impact of genetic heterogeneity on susceptibility to infection by pathogenic organisms in different mouse strains.[29,50-52] Arguably microbial pathogens engage much complex interaction with the host immune systems compared to nanomaterials with dramatic different outcomes; it is interesting to note that both carbon nanotubes and microbes could activate the NLRP3 inflammasome as an important component of the native immune response. Moreover, from a toxicological perspective, it is well-documented that genetic background determines the metabolic and injury responses of xenobiotics in whole organisms, ranging from bacteria to yeasts, vertebrates, mammals and humans etc.[29-30,51] Moreover, the toxicology literature also shows that for the same age and body weight, animals of different strains react differently with respect to the absorption, distribution, metabolism and secretion of xenobiotics and chemicals due to heterogeneous genetic effects.[53] This is confirmed by the findings in our study, which shows that genetic heterogeneity determines the differential expression of specific cytokines and growth factors such as IL-1β and TGF-β1, as well as the downstream biological effects that culminate in collagen deposition and fibrotic changes in the lung. These are examples of a large number of key biological factors, events and developmental stages during endothelial-mesenchymal transition (EMT), which shapes the lung fibrosis response in different mouse strains.[39-40] The EMT response is regulated by a host of biological pathways and response mechanisms that are under genetic control, including the assembly and involvement of the different components of the NLRP3 inflammasome, including the apoptosis-associated speck-like protein (ASC), pro-caspase 1 and the NLRP3 subunit.[42-43] Moreover, strain-specific variances in the activation of the inflammasome could also involve upstream pathways that signal the assembly of the NLRP3 inflammasome, including the lysosome response, cathepsin B release, oxidative stress generation (e.g., NADPH oxidase) and caspase 11 activation.[4] Familial Mediterranean fever (FMF) and Cryopyrin-associated periodic syndromes (CAPS) are examples of hereditary autoinflammatory diseases in humans that are determined by mutations in the MEFV and NLRP3 genes.[54] Moreover, downstream of the NLRP3 pathway, it is important to consider the influence of genetic heterogeneity on events such as TGF-β/Smad2 signal transduction and extracellular collagen deposition, as illustrated in idiopathic pulmonary fibrosis.[55] While detailed exploration of the above toxicogenomic responses are outside the scope of the current study, we expect that a great deal stands to be gained through further study of these response pathways in mouse strains. This knowledge can also be used for understanding the hazard of other LAR materials in the lung, such as nanowires.

The study also provides good proof-of-principle evidence to support the development of an adverse outcome pathway (AOP) approach for the hazard assessment of CNTs and other

nanomaterials. An AOP is a knowledge-based construct of existing and new data that describes a linear pathway, which commences with a molecular initiating event (MIE) that connects to an apical adverse outcome (AO) through a series of key events (KE)[40,56] Based on our previous studies on multi-wall and single-wall CNTs, we have delineated the key physicochemical properties and structure-activity relationships, allowing these materials to trigger lysosome damage and NLRP3 assembly as an example MIE.[3,8-9,16,31,36-37] Principally this involves physicochemical characteristics that determine bioavailability and lysosomal uptake, including the CNT length, state of aggregation, purity, surface coating, and colloidal stability, as well as a set of properties that determine surface catalytic activity leading to lysosomal damage in phagocytic cells, including metal impurities, catalytic surface reactivity, chirality, redox potential, and LAR.[3-4,8-9,17,36-37] Once damaged, the lysosomes release biological products such as cathepsin B, which in synergy with oxidative stress (e.g., NADPH oxidase) and perturbation of K^+ efflux, instructs assembly of the NLRP3 inflammasome and IL-1β production.[4,38] This constitutes an initial KE, which can be tested in primary macrophages or macrophage cell lines, as illustrated in this manuscript. Based on the AOP concept, a 2nd KE could be one of the events that take place in the epithelial cells, including TGF-β1 production or PDGF-AA production. Beyond this step, one can also envisage a KE that captures some of EMT responses, e.g., an assay that measures fibroblast proliferation or collagen deposition or possibly assessment of the TGF-β1 signal transduction pathway.[9,36-37] This communication describes the utility of IL-1β and TGF-β1 production in transformed cell lines or BMDMs to assess KE1 and KE2 responses for predicting a lung fibrosis AOP.[31,35]

There are potential shortcomings in this study. The 1st is that we use an oropharyngeal aspiration method, which leads to bolus dose exposure that is not representative of the slow cumulative increase in the lung burden during chronic inhalation exposure to powdered or dry MWCNTs.[12,57] However, since it has been reported that oropharyngeal or intratracheal instillation of CNTs do recapitulate some of the essential pathophysiology of inhalation exposure,[12] we attempted to use dosimetry calculations that has relevance to occupational exposures.[46] We also used a limited number of biomarkers for prediction-making that cannot possibly reflect the integrated complexity of sub-chronic lung inflammation and fibrosis.[39,58] To overcome this limitation, we propose a provisional AOP approach and a set of simple KE assays to initiate an early approach to CNT safety assessment while more comprehensive AOP constructs are being developed.[9,31] We also propose that toxicogenomics study tools can be used to develop a more complete picture of the gene responses, which will allow the introduction of further improved KEs.[59] It is also possible to identify genes that control the lung fibrosis phenotype in response to MWCNTs by quantitative trait locus mapping by identifying which molecular markers (e.g., SNPs or AFLPs) correlate with an observed trait. In addition to animal studies, we can also develop 3-D culture methods and stem cell-based lung organoids to develop non-vertebrate approaches to investigating MWCNT safety.[60]

CONCLUSION

In summary, we compare the susceptibility of MWCNT-induced pro-fibrogenic effects in different genetic backgrounds. The *ex vivo* screening using BMDMs from four mouse

strains demonstrated that the ranking order for IL-1β production, namely Balb/c > A/J > C57Bl/6 > NOD/ShiLtJ, was maintained in the lungs of intact animals during tracking of IL-1β, and TGF-β1 production in the BAL fluid or quantifying collagen deposition. Statistical analysis demonstrated good correlation between the *ex vivo* and *in vivo* data sets ranked according to the different strains. These findings indicate the predictive value of the *ex vivo* assays in BMDMs and portal-of-entry cell lines that reflect key biological events involved in a lung fibrosis AOP for MWCNTs. The strain dependence suggests the choice of mouse strain is an important consideration in planning CNT-induced lung toxicity studies.

MATERIALS AND METHODS

Source and Category of MWCNTs

The AP multi-walled carbon nanotube (MWCNT) samples, supplied by the NCNHIR consortium at the NIEHS, were purchased from Cheap Tubes, Inc. (Cambridge port, VT). The primary physicochemical characterization of these materials by the Nanotechnology Characterization Laboratory at the NCI described 3 size ranges: (i) 10-20 nm outer diameter with 0.5-2 μm lengths (NIEHS-12); (ii) 30-50 nm outer diameter with 0.5-2 μm lengths (NIEHS-13); and (iii) 10-20 nm outer diameter with 10-30 μm lengths (NIEHS-14). Two further variants of each type of 2 were derived by Prof. Somenath Mitra from the New Jersey Institute of Technology, namely: (i) carboxyl functionalized MWCNTs (NIEHS-12-2, NIEHS-13-2, NIEHS-14-2); and (ii) acid-purified MWCNTs (NIEHS-12-3, NIEHS-13-3, NIEHS-14-3). Altogether, this was provided as a library of 9 MWCNTs. The primary average lengths and diameters of the MWCNTs were assessed by TEM (JEOL 1200 EX transmission electron microscope). The elemental composition was determined by SEM-EDS (Hitachi S3000 scanning electron microscope). The hydrodynamic diameters of MWCNTs in H_2O and RPMI1640 were determined using high-throughput dynamic light scattering (HT-DLS, Dynapro Plate Reader) (Wyatt Technology, Santa Barbara, CA). The zeta (ζ) potentials of MWCNTs were determined using a ZetaSizer Nano-ZS (Malvern Instruments, Worcestershire WR, UK).

Chemicals and experimental materials

Bronchial epithelial growth medium (BEGM) was obtained from Lonza (Mapleton, IL, USA). BEGM is supplemented with a number of growth factors, including bovine pituitary extract, insulin, hydrocortisone, hEGF, epinephine, triiodothyronine, transferrin, gentamicin/amphotericin-B and retinoic acid. Roswell Park Memorial Institute medium 1640 (RPMI 1640) was purchased from Invitrogen (Carlsbad, CA, USA). Low-endotoxin bovine serum albumin (BSA) and fetal bovine serum (FBS) were from Gemini Bio-Products (West Sacramento, CA, USA). Dipalmitoylphosphatidylcholine (DPPC) was purchased from Sigma-Aldrich (St. Louis, MO, USA). Min-U-Sil was obtained from U.S. Silica (Frederick, MD, USA). All the MWCNT stock solutions were prepared using pure deionized water (DI H2O) with resistivity >18 Ω-cm.

Preparation of MWCNT suspensions and cell culture exposure

MWCNTs stock solutions were prepared in DI H_2O at 5 mg/mL. THP-1 cells were obtained from ATCC (Manassas, VA). THP-1 cells were pretreated with 1 μg/mL phorbol 12-

myristate acetate (PMA) overnight and primed with 10 ng/mL lipopolysaccharide (LPS). Aliquots of 3×10^4 primed cells were cultured in 0.1 mL medium with MWCNTs in 96-well plates (Costar, Corning, NY, USA) at 37 °C for 24 h. In order to provide less aggregated MWCNTs that can be suspended in biological aqueous media, all the MWCNT suspensions were freshly prepared by adding the stock solutions to RPMI 1640 media at 12.5 - 100 μg/mL in the presence of BSA (0.6 mg/mL) and DPPC (0.01 mg/mL).

Preparation of Bone Marrow-Derived Macrophages (BMDMs)

Bone marrow-derived macrophages (BMDMs) were prepared from the bone marrow of four different strains of mice, including C57Bl/6, Balb/c, NOD/SHILTJ and A/J, and cultured in 25% LADMAC conditioned medium as described previously. Briefly, femurs and tibia were cut on both ends and the marrow cavity was flushed with DMEM medium using a 5-mL syringe and 25-G needle. The cell suspension was repeatedly aspirated with a 10-mL pipet to disperse clumps. The cell suspension was then passed through a 70 μm cell strainer. Cells were spun down at 400 g for 10 min at 4 °C, and resuspended in 1 mL ice-cold 25% LADMAC conditioned medium. The cell concentration was adjusted to 10^6 cells/mL in 25% LADMAC conditioned medium and the cells were plated in 100 mm petri dishes. Cells were maintained for seven days at 37 °C. The medium was replaced with fresh 25% LADMAC every two days. After seven days, cells were dissociated from the plates using trypsin and re-plated at 5×10^4 cells/well in complete DMEM medium in a 96-well flat-bottom tissue culture plates. The well-established bone marrow-derived macrophages (BMDMs) were treated with 10 ng/mL recombinant murine IFN-γ for 48 h prior to use.

Determination of NLRP3 Inflammasome Activation and IL-1β Production

After 24 h of culture, the supernatants of MWCNT-exposed THP-1 cells were collected for the measurement of IL-1β (BD Biosciences, San Diego, CA) and TGF-β1 (Promega, Madison, WI), using ELISA kits according to manufacturer's instructions. Concentrations were expressed as pg/mL. For primary BMDMs, cells in 100 μL tissue culture medium were plated at the density of 5×10^4 per well in a 96-well plate with the addition of LPS (500 ng mL^{-1}) for 5 h. The medium was replaced with fresh media and the primed cells treated with MWCNTs at the doses of 12.5, 25, 50 and 100 μg/mL in the presence of LPS (10 ng/mL) for 24 h. The supernatants of the exposed cells were collected for IL-1β assessment.

Mouse exposure and assessment of exposure outcomes

Eight-week-old male C57Bl/6, Balb/c, NOD/SHILTJ and A/J mice were purchased from Charles River Laboratories (Hollister, CA). All animals were housed under standard laboratory conditions according to UCLA guidelines for care and treatment, as well as using the NIH Guide for the Care and Use of Laboratory Animals in Research (DHEW78-23). The animal experiments were approved by the Chancellor's Animal Research Committee at UCLA and include standard operating procedures for animal housing (filter-topped cages; room temperature at 23 ± 2 °C; 60 % relative humidity; 12 h light, 12 h dark cycle) and hygiene status (autoclaved food and acidified water). Animal exposures to MWCNTs were carried out by an oropharyngeal aspiration method developed at NIOSH. The animals in experiment groups received oropharyngeal aspiration of MWCNT NIEHS-14-1 suspensions at 2 mg/Kg at the back of the tongue. The mice were sacrificed after 21 days to assess sub-

chronic effects. The bronchoalveolar lavage fluid (BALF) and lung tissue were collected for measurement of TGF-β1 and PDGF-AA levels, performance of Hematoxylin and Eosin (H&E) or Masson's trichrome staining and total collagen content in the lung.

Sircol's Collagen Assay

The right cranial lobe of each lung was suspended in PBS at around 50 mg tissue/mL and homogenized for 60 s with a tissue homogenizer (Fisher Scientific). Triton X-100 was added to 1% and the samples were incubated for 18 h at room temperature. Acetic acid was added to each sample to a final concentration of 0.5 M and incubated at room temperature for 90 min. Cellular debris was pelleted by centrifugation and the supernatant analyzed for total protein, using a BCA assay kit (Pierce/ThermoFisher Scientific) according to manufacturer's instructions. The Sircol soluble collagen assay kit (Biocolor Ltd., Carrickfergus, UK) was used to extract collagen from duplicate samples using 200 μL supernatant and 800 μL Sircol dye reagent according to the manufacturer's instructions. Similar prepared collagen standards (10 50 μg) were run in parallel. Collagen pellets were washed twice with denatured alcohol and dried before suspension in alkali reagent. Absorbance at 540 nm was read on a plate reader (SpectroMax M5e, Molecular Devices Corp., Sunnyvale, CA). Data were expressed as micrograms of soluble collagen per milligrams of total protein.

Statistical Analysis

Mean and standard deviation (SD) was calculated for each parameter. Results were expressed as mean ± SD of multiple determinations. Comparisons within each group were conducted by a two-sided Student's t-test. A statistically significant difference was assumed with $p < 0.05$. Data from all endpoints for Figure 6 were log transformed to improve normality prior to analysis. Two-way analysis of variance (ANOVA) was performed to examine MWCNT treatment and mouse strain effects *ex vivo* and *in vivo*.

Supplementary Material

Refer to Web version on PubMed Central for supplementary material.

Acknowledgments

Research reported in this publication was supported by the National Institute of Environmental Health Sciences at the National Institutes of Health, under Award Numbers: U19 ES019528 (UCLA Center for NanoBiology and Predictive Toxicology), U01ES027237 and RO1ES022698. Leveraged support for characterization equipment used in this study was provided by the National Science Foundation and the Environmental Protection Agency, under Award No. DBI-1266377. Fluorescent microscopy was performed at the CNSI Advanced Light Microscopy/ Spectroscopy Shared Facility at UCLA.

References

1. De Volder MFL, Tawfick SH, Baughman RH, Hart AJ. Carbon Nanotubes: Present and Future Commercial Applications. Science. 2013; 339:535–539. [PubMed: 23372006]
2. Nel AE, Madler L, Velegol D, Xia T, Hoek EMV, Somasundaran P, Klaessig F, Castranova V, Thompson M. Understanding biophysicochemical interactions at the nano-bio interface. Nat Mater. 2009; 8:543–557. [PubMed: 19525947]
3. Wang X, Xia T, Duch M, Ji Z, Zhang H, Li R, Sun B, Lin S, Meng H, Liao YP, Wang M, Song TB, Yang Y, Hersam M, Nel A. Pluronic F108 Coating Decreases the Lung Fibrosis Potential of

Multiwall Carbon Nanotubes by Reducing Lysosomal Injury. Nano Letters. 2012; 12:3050–3061. [PubMed: 22546002]

4. Sun B, Wang X, Ji Z, Wang M, Liao YP, Chang CH, Li R, Zhang H, Nel AE, Xia T. NADPH Oxidase-Dependent NLRP3 Inflammasome Activation and its Important Role in Lung Fibrosis by Multiwalled Carbon Nanotubes. Small (Weinheim an der Bergstrasse, Germany). 2015; 11:2087–97.
5. Lin S, Wang X, Ji Z, Chang CH, Dong Y, Meng H, Liao YP, Wang M, Song TB, Kohan S, Xia T, Zink JI, Lin S, Nel AE. Aspect Ratio Plays a Role in the Hazard Potential of CeO2 Nanoparticles in Mouse Lung and Zebrafish Gastrointestinal Tract. Acs Nano. 2014; 8:4450–4464. [PubMed: 24720650]
6. Bonner J. Carbon nanotubes as a potential cause of pleural and interstitial lung diseases. Abstr Pap Am Chem S. 2012:244.
7. Shvedova AA, Pietroiusti A, Fadeel B, Kagan VE. Mechanisms of carbon nanotube-induced toxicity: Focus on oxidative stress. Toxicol Appl Pharm. 2012; 261:121–133.
8. Wang X, Mansukhani ND, Guiney LM, Lee JH, Li RB, Sun BB, Liao YP, Chang CH, Ji ZX, Xia T, Hersam MC, Nel AE. Toxicological Profiling of Highly Purified Metallic and Semiconducting Single-Walled Carbon Nanotubes in the Rodent Lung and E. coli. ACS Nano. 2016; 10:6008–6019. [PubMed: 27159184]
9. Wang X, Duch MC, Mansukhani N, Ji Z, Liao YP, Wang M, Zhang H, Sun B, Chang CH, Li R, Lin S, Meng H, Xia T, Hersam MC, Nel AE. Use of a Pro-Fibrogenic Mechanism-Based Predictive Toxicological Approach for Tiered Testing and Decision Analysis of Carbonaceous Nanomaterials. ACS Nano. 2015; 9:3032–3043. [PubMed: 25646681]
10. Wang LY, Mercer RR, Rojanasakul Y, Qiu AJ, Lu YJ, Scabilloni JF, Wu NQ, Castranova V. Direct Fibrogenic Effects of Dispersed Single-Walled Carbon Nanotubes on Human Lung Fibroblasts. J Toxicol Env Heal A. 2010; 73:410–422.
11. Shvedova AA, Kisin ER, Mercer R, Murray AR, Johnson VJ, Potapovich AI, Tyurina YY, Gorelik O, Arepalli S, Schwegler-Berry D, Hubbs AF, Antonini J, Evans DE, Ku BK, Ramsey D, Maynard A, Kagan VE, Castranova V, Baron P. Unusual inflammatory and fibrogenic pulmonary responses to single-walled carbon nanotubes in mice. Am J Physiol-Lung C. 2005; 289:L698–L708.
12. Shvedova AA, Kisin E, Murray AR, Johnson VJ, Gorelik O, Arepalli S, Hubbs AF, Mercer RR, Keohavong P, Sussman N, Jin J, Yin J, Stone S, Chen BT, Deye G, Maynard A, Castranova V, Baron PA, Kagan VE. Inhalation vs. aspiration of single-walled carbon nanotubes in C57BL/6 mice: inflammation, fibrosis, oxidative stress, and mutagenesis. Am J Physiol-Lung C. 2008; 295:L552–L565.
13. Ryman-Rasmussen JP, Tewksbury EW, Moss OR, Cesta MF, Wong BA, Bonner JC. Inhaled Multiwalled Carbon Nanotubes Potentiate Airway Fibrosis in Murine Allergic Asthma. Am J Resp Cell Mol. 2009; 40:349–358.
14. Mutlu GM, Budinger GRS, Green AA, Urich D, Soberanes S, Chiarella SE, Alheid GF, McCrimmon DR, Szleifer I, Hersam MC. Biocompatible Nanoscale Dispersion of Single-Walled Carbon Nanotubes Minimizes in vivo Pulmonary Toxicity. Nano Letters. 2010; 10:1664–1670. [PubMed: 20377197]
15. Murthy PB, Kishore AS, Surekha P. Acute Toxicological Effects of Multi-Walled Carbon Nanotubes (MWCNT). Carbon Nanotubes - Growth and Applications. 2011:529–538.
16. Liu AH, Sun KN, Yang JF, Zhao DM. Toxicological effects of multi-wall carbon nanotubes in rats. J Nanopart Res. 2008; 10:1303–1307.
17. Li R, Wang X, Ji Z, Sun B, Zhang H, Chang CH, Lin S, Meng H, Liao YP, Wang M, Li Z, Hwang AA, Song TB, Xu R, Yang Y, Zink JI, Nel AE, Xia T. Surface charge and cellular processing of covalently functionalized multiwall carbon nanotubes determine pulmonary toxicity. ACS Nano. 2013; 7:2352–68. [PubMed: 23414138]
18. Hamilton RF, Wu NQ, Porter D, Buford M, Wolfarth M, Holian A. Particle length-dependent titanium dioxide nanomaterials toxicity and bioactivity. Particle and Fibre Toxicology. 2009; 6
19. Dostert C, Petrilli V, Van Bruggen R, Steele C, Mossman BT, Tschopp J. Innate Immune Activation through Nalp3 Inflammasome Sensing of Asbestos and Silica. Science. 2008; 320:674–677. [PubMed: 18403674]

20. Chen T, Nie HY, Gao X, Yang JL, Pu J, Chen ZJ, Cui XX, Wang Y, Wang HF, Jia G. Epithelial-mesenchymal transition involved in pulmonary fibrosis induced by multi-walled carbon nanotubes via TGF-beta/Smad signaling pathway. Toxicol Lett. 2014; 226:150–162. [PubMed: 24530353]
21. Bonner JC, Silva RM, Taylor AJ, Brown JM, Hilderbrand SC, Castranova V, Porter D, Elder A, Oberdorster G, Harkema JR, Bramble LA, Kavanagh TJ, Botta D, Nel A, Pinkerton KE. Interlaboratory Evaluation of Rodent Pulmonary Responses to Engineered Nanomaterials: The NIEHS Nano GO Consortium. Environmental Health Perspectives. 2013; 121:676–682. [PubMed: 23649427]
22. Mishra A, Stueckle TA, Mercer RR, Derk R, Rojanasakul Y, Castranova V, Wang LY. Identification of TGF-beta receptor-1 as a key regulator of carbon nanotube-induced fibrogenesis. Am J Physiol-Lung C. 2015; 309:L821–L833.
23. Guarnieri M, Balmes JR. Outdoor air pollution and asthma. Lancet. 2014; 383:1581–1592. [PubMed: 24792855]
24. Scoville DK, White CC, Botta D, McConnachie LA, Zadworny ME, Schmuck SC, Hu XG, Gao XH, Yu JB, Dills RL, Sheppard L, Delaney MA, Griffith WC, Beyer RP, Zangar RC, Pounds JG, Faustman EM, Kavanagh TJ. Susceptibility to quantum dot induced lung inflammation differs widely among the Collaborative Cross founder mouse strains. Toxicol Appl Pharm. 2015; 289:240–250.
25. Lucas RM, Norval M, Neale RE, Young AR, de Gruijl FR, Takizawa Y, van der Leun JC. The consequences for human health of stratospheric ozone depletion in association with other environmental factors. Photoch Photobio Sci. 2015; 14:53–87.
26. Fathy M, Hamed M, Youssif O, Fawzy N, Ashour W. Association Between Environmental Tobacco Smoke Exposure and Lung Cancer Susceptibility: Modification by Antioxidant Enzyme Genetic Polymorphisms. Mol Diagn Ther. 2014; 18:55–62. [PubMed: 23928928]
27. Schroder A, Klein K, Winter S, Schwab M, Bonin M, Zell A, Zanger UM. Genomics of ADME gene expression: mapping expression quantitative trait loci relevant for absorption, distribution, metabolism and excretion of drugs in human liver. Pharmacogenomics J. 2013; 13:12–20. [PubMed: 22006096]
28. Du YX, Xu XH, Chu M, Guo Y, Wang JH. Air particulate matter and cardiovascular disease: the epidemiological, biomedical and clinical evidence. J Thorac Dis. 2016; 8:E8–E19. [PubMed: 26904258]
29. Hunter DJ. Gene-environment interactions in human diseases. Nature reviews Genetics. 2005; 6:287–98.
30. Schwartz DA. The importance of gene-environment interactions and exposure assessment in understanding human diseases. Journal of exposure science & environmental epidemiology. 2006; 16:474–6. [PubMed: 17109021]
31. Godwin H, Nameth C, Avery D, Bergeson LL, Bernard D, Beryt E, Boyes W, Brown S, Clippinger AJ, Cohen Y, Doa M, Hendren CO, Holden P, Houck K, Kane AB, Klaessig F, Kodas T, Landsiedel R, Lynch I, Malloy T, Miller MB, Muller J, Oberdorster G, Petersen EJ, Pleus RC, Sayre P, Stone V, Sullivan KM, Tentschert J, Wallis P, Nel AE. Nanomaterial Categorization for Assessing Risk Potential To Facilitate Regulatory Decision-Making. ACS Nano. 2015; 9:3409–3417. [PubMed: 25791861]
32. Nel A, Xia T, Meng H, Wang X, Lin S, Ji Z, Zhang H. Nanomaterial Toxicity Testing in the 21st Century: Use of a Predictive Toxicological Approach and High-Throughput Screening. Accounts of Chemical Research. 2013; 46:607–621. [PubMed: 22676423]
33. Trasande L. Updating the Toxic Substances Control Act to Protect Human Health. Jama-J Am Med Assoc. 2016; 315:1565–1566.
34. Wilson J, Ogunseitan OA. A Call for Better Toxics Policy Reform. Environment. 2017; 59:30–33.
35. Nel AE, Nasser E, Godwin H, Avery D, Bahadori T, Bergeson L, Beryt E, Bonner JC, Boverhof D, Carter J, Castranova V, DeShazo JR, Hussain SM, Kane AB, Klaessig F, Kuempel E, Lafranconi M, Landsiedel R, Malloy T, Miller MB, Morris J, Moss K, Oberdorster G, Pinkerton K, Pleus RC, Shatkin JA, Thomas R, Tolaymat T, Wang A, Wong J. A Multi-Stakeholder Perspective on the Use of Alternative Test Strategies for Nanomaterial Safety Assessment. ACS Nano. 2013; 7:6422–6433. [PubMed: 23924032]

36. Wang X, Xia T, Ntim SA, Ji Z, George S, Meng H, Zhang H, Castranova V, Mitra S, Nel AE. Quantitative techniques for assessing and controlling the dispersion and biological effects of multiwalled carbon nanotubes in mammalian tissue culture cells. ACS Nano. 2010; 4:7241–52. [PubMed: 21067152]
37. Wang X, Xia T, Addo Ntim S, Ji Z, Lin S, Meng H, Chung C-H, George S, Zhang H, Wang M, Li N, Yang Y, Castranova V, Mitra S, Bonner JC, Nel AE. Dispersal State of Multiwalled Carbon Nanotubes Elicits Profibrogenic Cellular Responses That Correlate with Fibrogenesis Biomarkers and Fibrosis in the Murine Lung. ACS Nano. 2011; 5:9772–9787. [PubMed: 22047207]
38. Sun BB, Wang X, Ji ZX, Li RB, Xia T. NLRP3 Inflammasome Activation Induced by Engineered Nanomaterials. Small. 2013; 9:1595–1607. [PubMed: 23180683]
39. Bonner JC. Mesenchymal cell survival in airway and interstitial pulmonary fibrosis. Fibrogenesis & tissue repair. 2010; 3:15. [PubMed: 20738867]
40. Vietti G, Lison D, van den Brule S. Mechanisms of lung fibrosis induced by carbon nanotubes: towards an Adverse Outcome Pathway (AOP). Particle and Fibre Toxicology. 2016:13. [PubMed: 26956024]
41. Strowig T, Henao-Mejia J, Elinav E, Flavell R. Inflammasomes in Health and Disease. Nature. 2012; 481:278–286. [PubMed: 22258606]
42. Schroder K, Zhou RB, Tschopp J. The NLRP3 Inflammasome: A Sensor for Metabolic Danger? Science. 2010; 327:296–300. [PubMed: 20075245]
43. Schroder K, Tschopp J. The Inflammasomes. Cell. 2010; 140:821–832. [PubMed: 20303873]
44. Simecek P, Churchill GA, Yang H, Rowe LB, Herberg L, Serreze DV, Leiter EH. Genetic Analysis of Substrain Divergence in Non-Obese Diabetic (NOD) Mice. G3-Genes Genom Genet. 2015; 5:771–775.
45. Xia TA, Zhao Y, Sager T, George S, Pokhrel S, Li N, Schoenfeld D, Meng HA, Lin SJ, Wang X, Wang MY, Ji ZX, Zink JI, Madler L, Castranova V, Lin S, Nel AE. Decreased Dissolution of ZnO by Iron Doping Yields Nanoparticles with Reduced Toxicity in the Rodent Lung and Zebrafish Embryos. ACS Nano. 2011; 5:1223–1235. [PubMed: 21250651]
46. Han JH, Lee EJ, Lee JH, So KP, Lee YH, Bae GN, Lee SB, Ji JH, Cho MH, Yu IJ. Monitoring multiwalled carbon nanotube exposure in carbon nanotube research facility. Inhal Toxicol. 2008; 20:741–749. [PubMed: 18569096]
47. Wang X, Ji ZX, Chang CH, Zhang HY, Wang MY, Liao YP, Lin SJ, Meng H, Li RB, Sun BB, Winkle LV, Pinkerton KE, Zink JI, Xia T, Nel AE. Use of Coated Silver Nanoparticles to Understand the Relationship of Particle Dissolution and Bioavailability to Cell and Lung Toxicological Potential. Small. 2014; 10:385–398. [PubMed: 24039004]
48. Han, J., Kamber, M., Pei, J. Morgan Kaufmann series in data management systems. 3. Morgan Kaufmann/Elsevier; Waltham, MA: 2012. Safari Books Online (Firm): Data mining concepts and techniques.
49. Wakefield, J. Bayesian and Frequentist regression methods. Springer; 2012.
50. Zaragoza O, Alvarez M, Telzak A, Rivera J, Casadevall A. The relative susceptibility of mouse strains to pulmonary Cryptococcus neoformans infection is associated with pleiotropic differences in the immune response. Infect Immun. 2007; 75:2729–2739. [PubMed: 17371865]
51. Marques SM, Campos PP, Castro PR, Cardoso CC, Ferreira MAND, Andrade SP. Genetic background determines mouse strain differences in inflammatory angiogenesis. Microvasc Res. 2011; 82:246–252. [PubMed: 21907724]
52. Packiam M, Veit SJ, Anderson DJ, Ingalls RR, Jerse AE. Mouse Strain-Dependent Differences in Susceptibility to Neisseria gonorrhoeae Infection and Induction of Innate Immune Responses. Infect Immun. 2010; 78:433–440. [PubMed: 19901062]
53. Gochfeld M. Sex Differences in Human and Animal Toxicology. Toxicol Pathol. 2017; 45:172–189. [PubMed: 27895264]
54. Bozkurt Y, Demir A, Erman B, Gul A. Unified Modeling of Familial Mediterranean Fever and Cryopyrin Associated Periodic Syndromes. Comput Math Method M. 2015
55. Fernandez IE, Eickelberg O. The impact of TGF-beta on lung fibrosis: from targeting to biomarkers. Proc Am Thorac Soc. 2012; 9:111–6. [PubMed: 22802283]

56. Vinken M. The adverse outcome pathway concept: A pragmatic tool in toxicology. Toxicology. 2013; 312:158–165. [PubMed: 23978457]

57. Guttenberg M, Bezerra L, Neu-Baker NM, Idelchik MDS, Elder A, Oberdorster G, Brenner SA. Biodistribution of inhaled metal oxide nanoparticles mimicking occupational exposure: a preliminary investigation using enhanced darkfield microscopy. J Biophotonics. 2016; 9:987–993. [PubMed: 27528427]

58. Renzoni E, Srihari V, Sestini P. Pathogenesis of idiopathic pulmonary fibrosis: review of recent findings. F1000prime reports. 2014; 6:69. [PubMed: 25165568]

59. Aardema MJ, MacGregor JT. Toxicology and genetic toxicology in the new era of "toxicogenomics": impact of "-omics" technologies. Mutat Res-Fund Mol M. 2002; 499:13–25.

60. Sanchez VC, Weston P, Yan AH, Hurt RH, Kane AB. A 3-dimensional in vitro model of epithelioid granulomas induced by high aspect ratio nanomaterials. Particle and Fibre Toxicology. 2011; 8

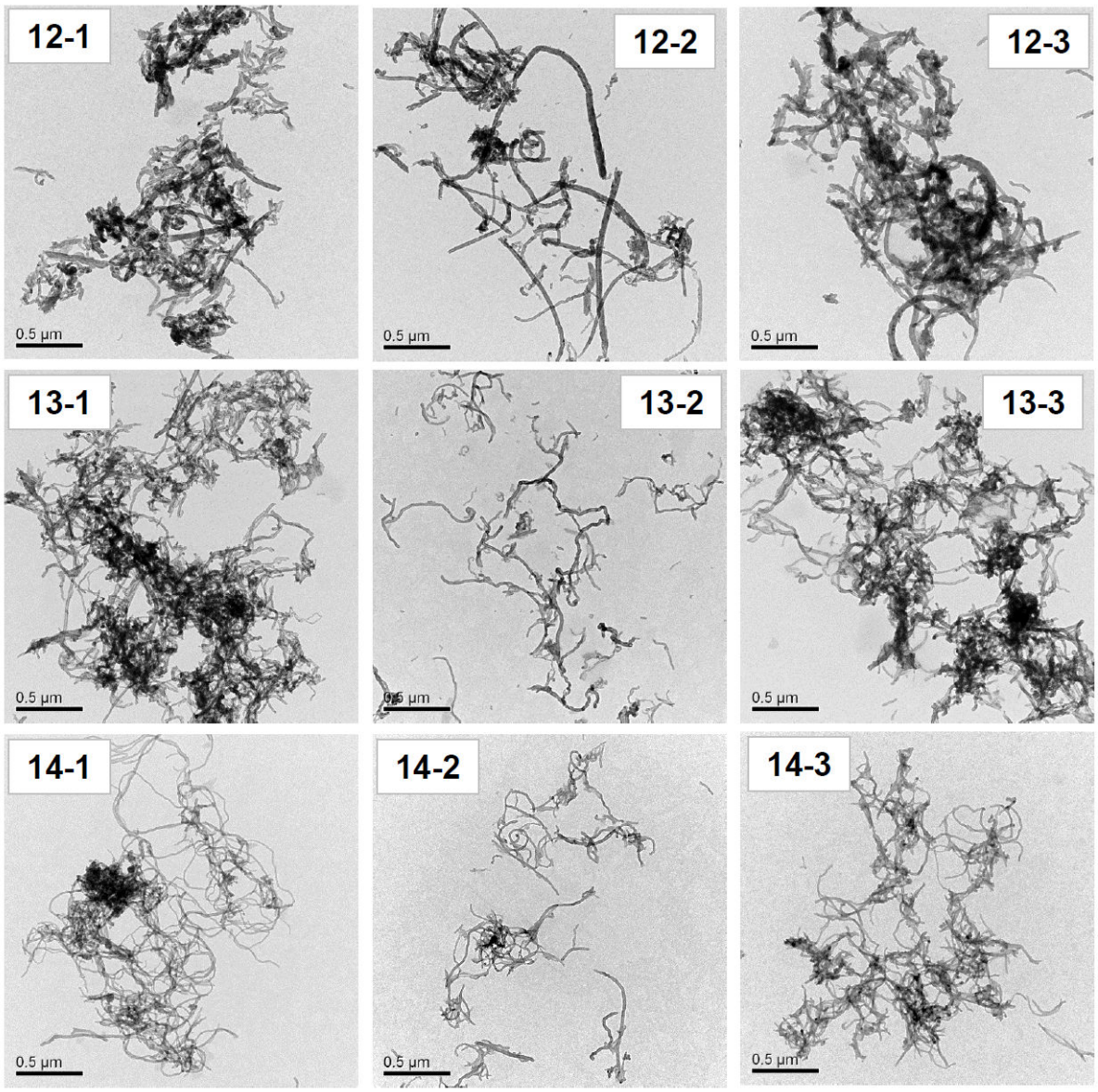

Figure 1. Representative transmission electron microscopy (TEM) images of the MWCNT library

TEM images were acquired using a JEOL 1200 EX TEM (JEOL 1200 EX transmission electron microscope).

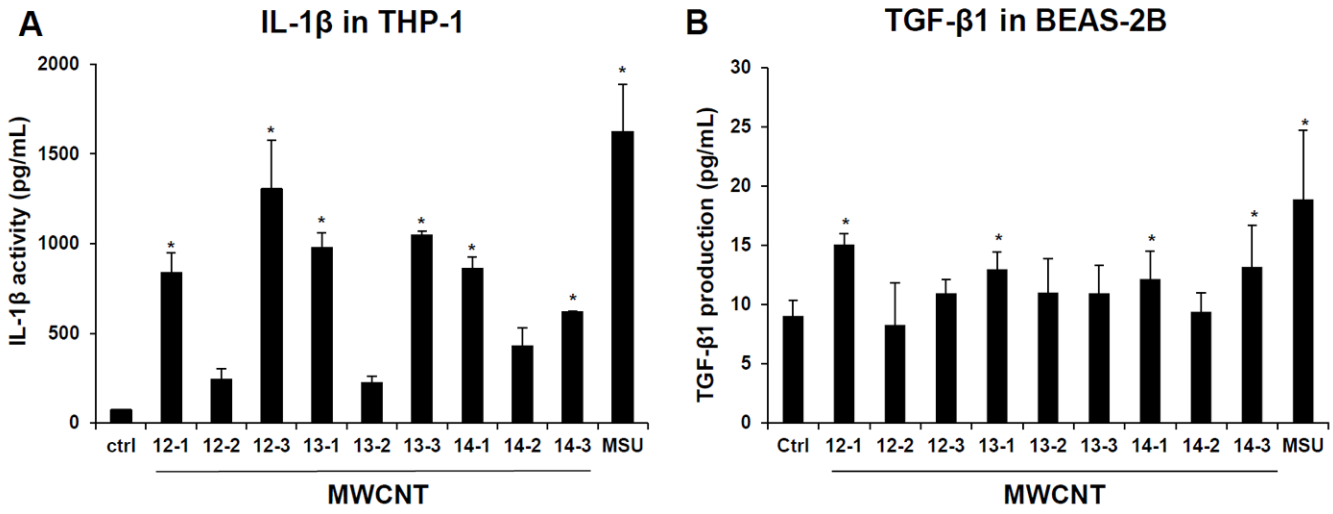

Figure 2. MWCNT induced IL-1β and TGF-β1 production in THP-1 and BEAS-2B tissue culture cells

Both cell types were grown in 96-well plates, followed by exposure to 12.5, 25, 50 and 100 μg/mL of each of the MWNCTs suspensions for 24 h. IL-1β (A) and TGF-β1 (B) levels were determined by ELISA, using the supernatants of treated THP-1 and BEAS-2B cells respectively. MSU was used as positive control. *$p < 0.05$ compared to control.

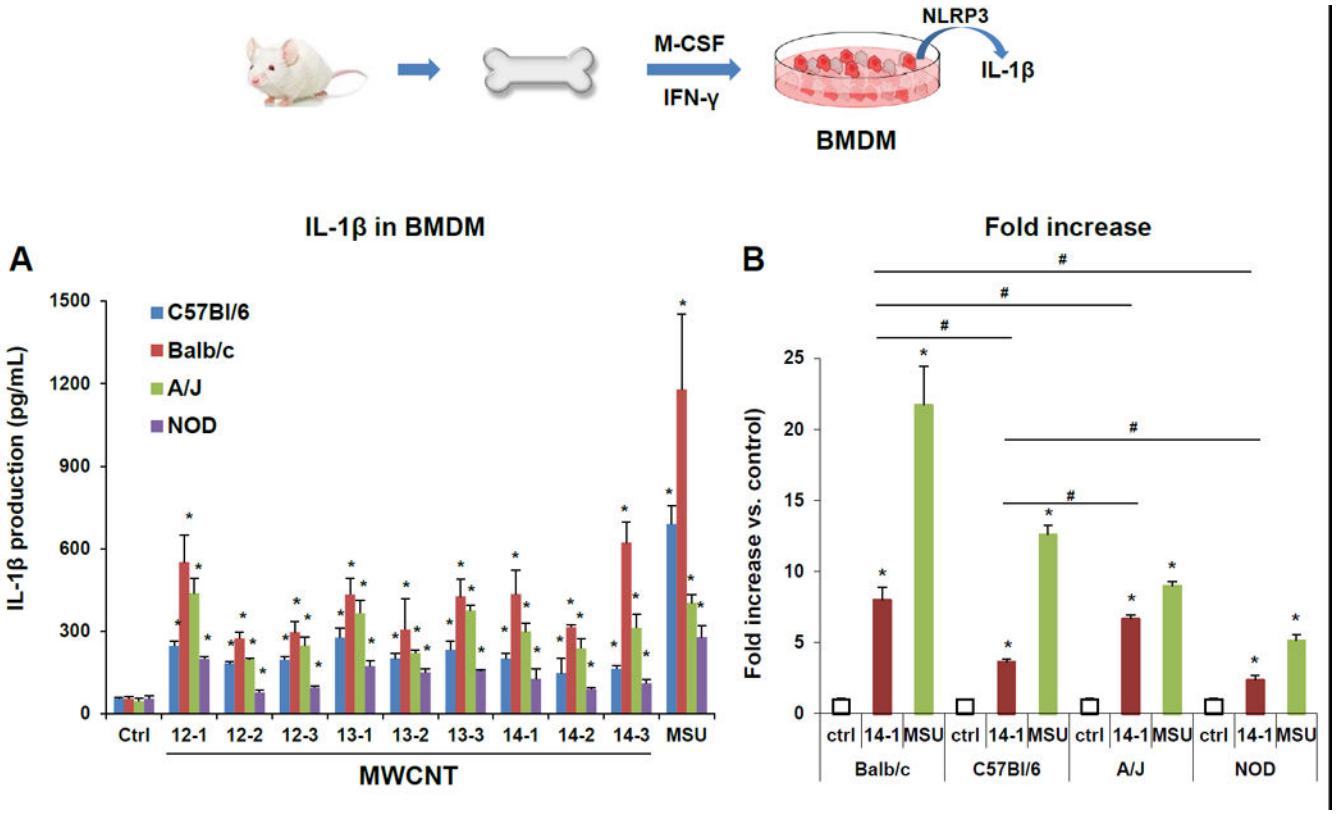

Figure 3. Comparison of MWCNT-induced IL-1β production in BMDM cells

BMDMs were derived from four mouse strains, C57Bl/6, Balb/c, NOD/ShiLtJ and A/J, which were exposed to MWCNT samples at doses of 12.5, 25, 50 and 100 μg/mL (detailed method can be found in the Method section) for 24 h. IL-1β production levels (A) and the fold increase in relationship to non-treated cells (B) were determined by ELISA, using the cellular supernatants. *p< 0.05 compared to control; # p< 0.05 compared between different strains.

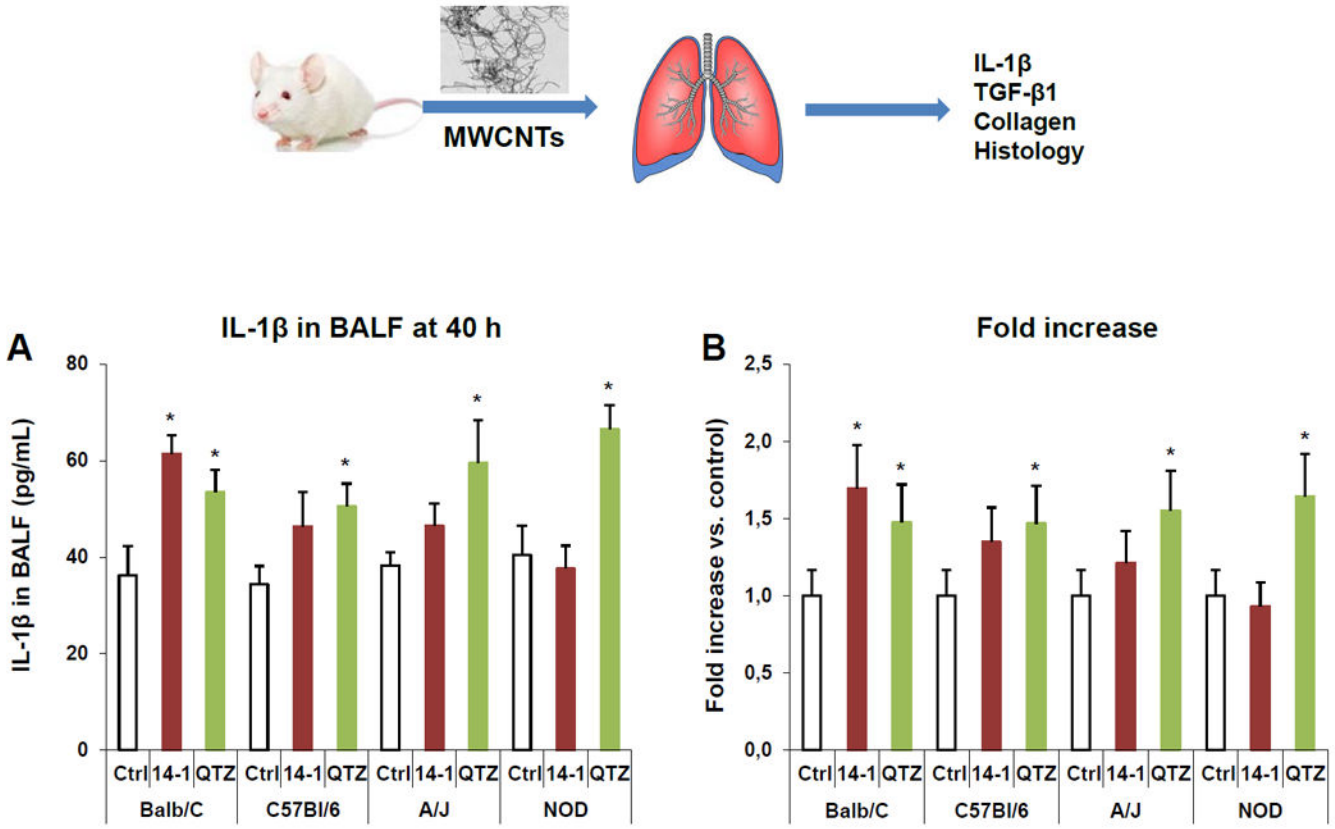

Figure 4. Assessment of the IL-1β production after 40 h in the respective mouse strains

Anesthetized mice were individually weighed and exposed to MWNCTs (14-1), delivered by one-time oropharyngeal aspiration at 2.0 mg/kg. MWCNT sample 14-1 was selected because it has low endotoxin contamination and induced high cytokine production *in vitro*. Animals were euthanized after 40 h, and BALF was collected to determine IL-1β levels by ELISA (A), which was also expressed as fold-increase, with respect to non-treated animals (B). *p< 0.05 compared to control; # p< 0.05 for inter-strain comparison.

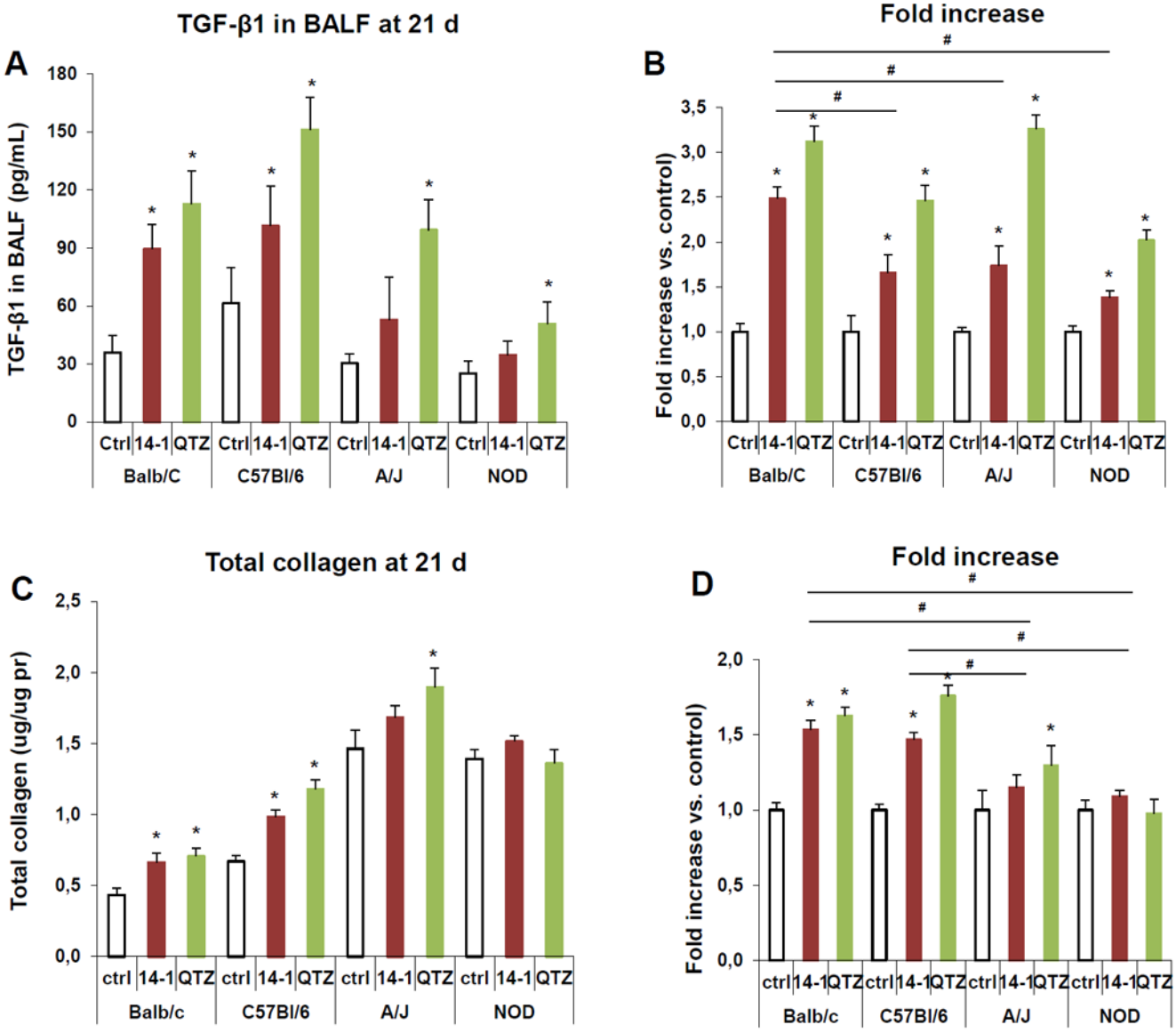

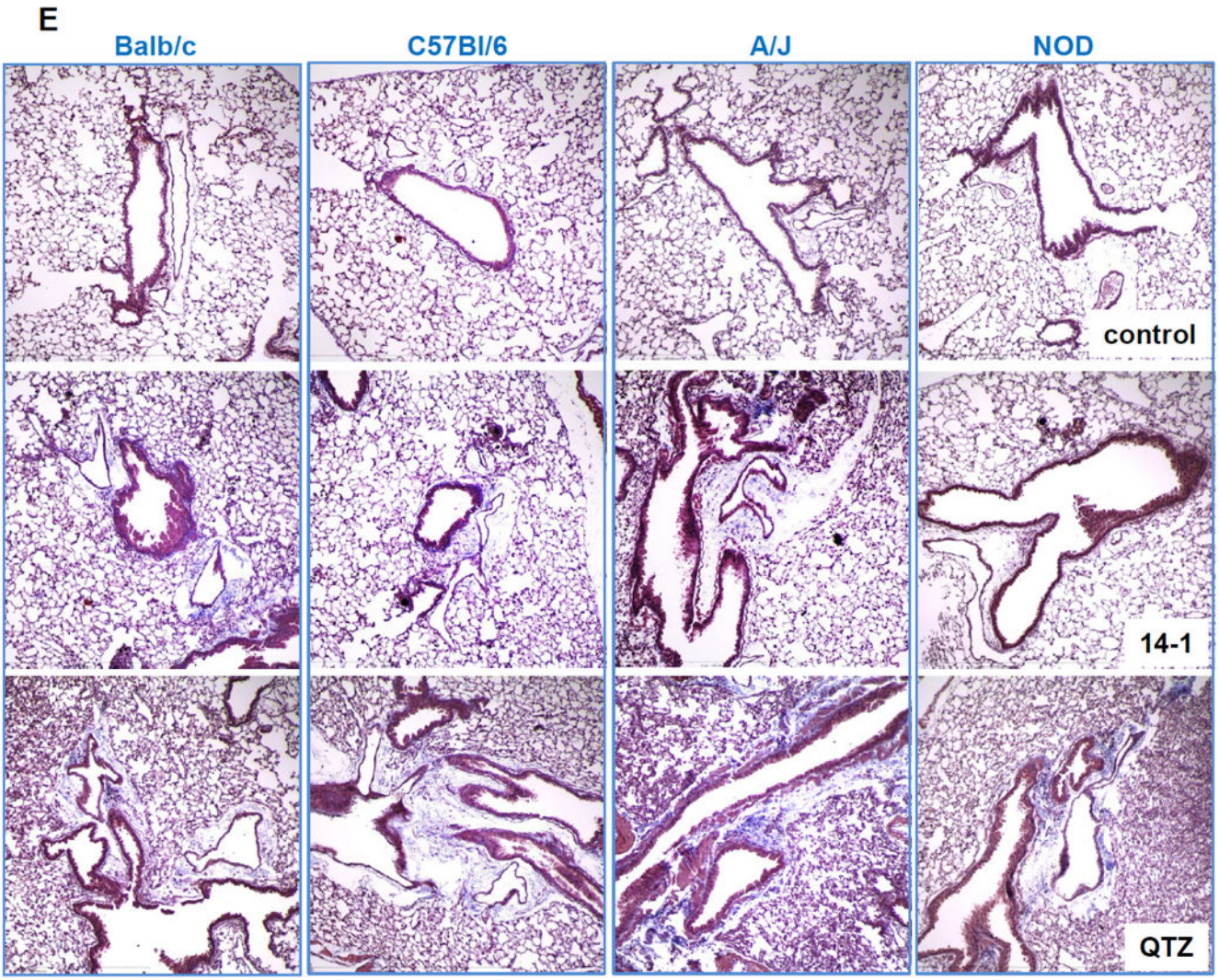

Figure 5. Assessment of the pro-fibrogenic effects of MWNCTs in the respective mouse strains after 21 days

Anesthetized mice were weighed individually and exposed to the same dose of MWNCTs as in Figure 4. Animals were euthanized after 21 days, and BALF was collected to determine TGF-β1 (A) levels by ELISA. The same data was also expressed as fold increase compared to non-treated animals (B). Total collagen content (C and D) of the lung tissue was determined by a Sircol collagen kit (Biocolor Ltd., Carrickfergus, UK). Histological evidence of collagen deposition in the same animals' lungs was determined by Masson's trichrome staining and observed at 100 × magnification (E). Collagen staining appears as a blue color. Animals exposed to Quartz (QTZ) served as positive control. *$p < 0.05$ compared to control; # $p < 0.05$ for inter-strain comparison.

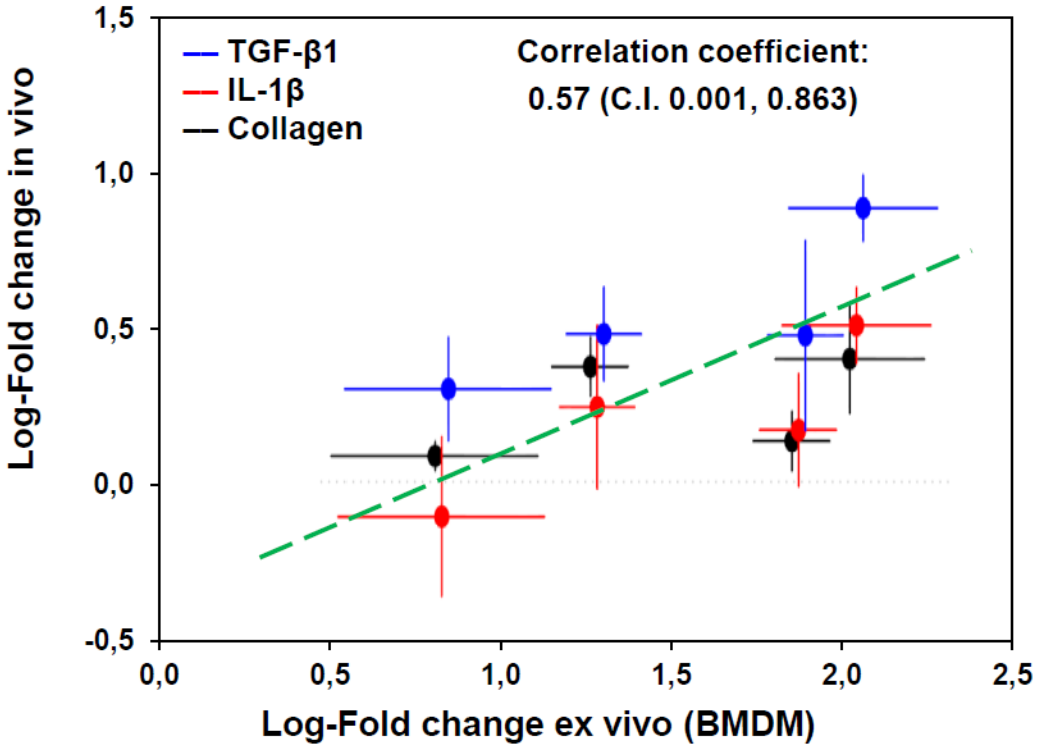

Figure 6. Statistical correlation between BMDM-derived *ex vivo* data and animal lung data *in vivo*

Log-fold change of BMDM IL-1β *ex vivo* vs. log-fold change of *in vivo* endpoints for all mouse strains. Each point represents the estimated mean effect. For each point, we report the associated 95% confidence intervals in both dimensions.

Table 1

Physicochemical Characterization of MWCNTs.

MWCNTs		Primary Size		Element composition (wt%)				ζ potential (mV)		Hydrodynamic size (nm)	
		Diameter	Length	C	O	Ni	Fe	H2O	RPMI	H2O	RPMI
12-1	AP-			94.1± 0.7	4.7±0.7	0.8 ± 0.7	0.4 ± 0.3	-20.3 ± 0.6	-11.9 ± 2.3	226.6 ± 1.8	418.9 ± 16
12-2	COOH-	10-20 nm	0.5-2 μm	92.2±0.8	6.7±0.3	0.7±0.8	0.4 ± 0.4	-49.4 ± 1.7	-14.6 ± 2.2	131.4 ± 3.4	237.7 ± 6.
12-3	PD-			93.5±0.3	4.6±0.2	1.4±0.2	0.5±0.2	-22.4 ± 1.0	-13.1 ± 3.2	231.0 ± 1.8	350.2 ± 7.
13-1	AP-			94.1± 0.5	4.5±0.4	1.1±0.8	0.3±0.2	-19.8 ± 0.6	-10.3 ± 2.9	650.9 ± 17.0	571.5 ± 14
13-2	COOH-	30-50 nm	0.5-2 μm	88.6±2.6	8.0±0.8	2.3±2.5	0.9±1.0	-54.4 ± 0.7	-15.8 ± 3.4	171.7 ± 2.6	247.2 ± 3.
13-3	PD-			94.9± 0.8	3.3±0.3	1.2±0.9	0.7±0.2	-25.2 ± 0.8	-11.7 ± 2.5	345.8 ± 11.1	582.8 ± 8.
14-1	AP-			95.8± 0.6	3.4±0.2	0.5±0.5	0.3±0.3	-26.9 ± 1.1	-12.7 ± 1.0	292.9 ± 6.3	647.4 ± 30
14-2	COOH-	10-20 nm	10-30 μm	91.8±0.4	7.4±0.5	0.5±0.5	0.3±0.4	-53.0 ± 1.7	-16.0 ± 1.3	105.8 ± 0.6	220.1 ± 3.
14-3	PD-			95.9±0.4	2.9±1.4	0.2±0.5	0.3±0.3	-23.4 ± 0.4	-10.5 ± 0.9	442.8 ± 14.6	690.4 ± 28

The average lengths and diameters of the MWCNTs were assessed by TEM JEOL 1200 EX TEM (JEOL 1200 EX transmission electron microscope). The elemental composition was determined by SEM-EDS (Hitachi S3000 scanning electron microscope). The zeta potential was measured using a ZetaSizer Nano-ZS (Malvern Instruments, Worcestershire WR, U.K.). The hydrodynamic diameters in H_2O and RPMI1640 were determined using high-throughput dynamic light scattering (HT-DLS, Dynapro Plate Reader, Wyatt Technology).

Table 2

Two-way ANOVA of strain by biological outcome

	Df	Sum Sq	Mean Sq	F value	P (>F)
Outcome	3	16.088	5.363	104.298	0.000
Strain	3	4.032	1.344	26.140	0.000
Interaction (Outcome Strain)	9	1.733	0.193	3.744	0.001
Residuals	68	3.496	0.051	NA	NA

Two-way analysis of variance (ANOVA) was performed to examine MWCNT treatment and mouse strain effects *ex vivo* and *in vivo*. In the first column, the terminology refers to 1) Outcome: biological outcomes obtained in *ex vivo* and *in vivo* assays, including the IL-1β production in BMDMs (*ex vivo*), IL-1β, TGF-β1 production in BAL fluid and collagen content in the lung; 2) Strain: the four mouse strains we studied in this study; 3) Interaction (Outcome:Strain): the interaction between the features of outcome and strain; 4) Residuals: the amount of unexplained variation. Df: degree of freedom; Sq: square.